Search for Long-Lived Particles in e^+e^- Collisions

J. P. Lees,[1] V. Poireau,[1] V. Tisserand,[1] E. Grauges,[2] A. Palano,[3a,3b] G. Eigen,[4] B. Stugu,[4] D. N. Brown,[5] L. T. Kerth,[5] Yu. G. Kolomensky,[5] M. J. Lee,[5] G. Lynch,[5] H. Koch,[6] T. Schroeder,[6] C. Hearty,[7] T. S. Mattison,[7] J. A. McKenna,[7] R. Y. So,[7] A. Khan,[8] V. E. Blinov,[9a,9b,9c] A. R. Buzykaev,[9a] V. P. Druzhinin,[9a,9b] V. B. Golubev,[9a,9b] E. A. Kravchenko,[9a,9b] A. P. Onuchin,[9a,9b,9c] S. I. Serednyakov,[9a,9b] Yu. I. Skovpen,[9a,9b] E. P. Solodov,[9a,9b] K. Yu. Todyshev,[9a,9b] A. J. Lankford,[10] B. Dey,[11] J. W. Gary,[11] O. Long,[11] C. Campagnari,[12] M. Franco Sevilla,[12] T. M. Hong,[12] D. Kovalskyi,[12] J. D. Richman,[12] C. A. West,[12] A. M. Eisner,[13] W. S. Lockman,[13] W. Panduro Vazquez,[13] B. A. Schumm,[13] A. Seiden,[13] D. S. Chao,[14] C. H. Cheng,[14] B. Echenard,[14] K. T. Flood,[14] D. G. Hitlin,[14] T. S. Miyashita,[14] P. Ongmongkolkul,[14] F. C. Porter,[14] M. Röhrken,[14] R. Andreassen,[15] Z. Huard,[15] B. T. Meadows,[15] B. G. Pushpawela,[15] M. D. Sokoloff,[15] L. Sun,[15] P. C. Bloom,[16] W. T. Ford,[16] A. Gaz,[16] J. G. Smith,[16] S. R. Wagner,[16] R. Ayad,[17,†] W. H. Toki,[17] B. Spaan,[18] D. Bernard,[19] M. Verderi,[19] S. Playfer,[20] D. Bettoni,[21a] C. Bozzi,[21a] R. Calabrese,[21a,21b] G. Cibinetto,[21a,21b] E. Fioravanti,[21a,21b] I. Garzia,[21a,21b] E. Luppi,[21a,21b] L. Piemontese,[21a] V. Santoro,[21a] A. Calcaterra,[22] R. de Sangro,[22] G. Finocchiaro,[22] S. Martellotti,[22] P. Patteri,[22] I. M. Peruzzi,[22,‡] M. Piccolo,[22] M. Rama,[22] A. Zallo,[22] R. Contri,[23a,23b] M. Lo Vetere,[23a,23b] M. R. Monge,[23a,23b] S. Passaggio,[23a] C. Patrignani,[23a,23b] E. Robutti,[23a] B. Bhuyan,[24] V. Prasad,[24] A. Adametz,[25] U. Uwer,[25] H. M. Lacker,[26] U. Mallik,[27] C. Chen,[28] J. Cochran,[28] S. Prell,[28] H. Ahmed,[29] A. V. Gritsan,[30] N. Arnaud,[31] M. Davier,[31] D. Derkach,[31] G. Grosdidier,[31] F. Le Diberder,[31] A. M. Lutz,[31] B. Malaescu,[31,§] P. Roudeau,[31] A. Stocchi,[31] G. Wormser,[31] D. J. Lange,[32] D. M. Wright,[32] J. P. Coleman,[33] J. R. Fry,[33] E. Gabathuler,[33] D. E. Hutchcroft,[33] D. J. Payne,[33] C. Touramanis,[33] A. J. Bevan,[34] F. Di Lodovico,[34] R. Sacco,[34] G. Cowan,[35] D. N. Brown,[36] C. L. Davis,[36] A. G. Denig,[37] M. Fritsch,[37] W. Gradl,[37] K. Griessinger,[37] A. Hafner,[37] K. R. Schubert,[37] R. J. Barlow,[38,‖] G. D. Lafferty,[38] R. Cenci,[39] B. Hamilton,[39] A. Jawahery,[39] D. A. Roberts,[39] R. Cowan,[40] G. Sciolla,[40] R. Cheaib,[41] P. M. Patel,[41,*] S. H. Robertson,[41] N. Neri,[42a] F. Palombo,[42a,42b] L. Cremaldi,[43] R. Godang,[43,¶] P. Sonnek,[43] D. J. Summers,[43] M. Simard,[44] P. Taras,[44] G. De Nardo,[45a,45b] G. Onorato,[45a,45b] C. Sciacca,[45a,45b] M. Martinelli,[46] G. Raven,[46] C. P. Jessop,[47] J. M. LoSecco,[47] K. Honscheid,[48] R. Kass,[48] E. Feltresi,[49a,49b] M. Margoni,[49a,49b] M. Morandin,[49a] M. Posocco,[49a] M. Rotondo,[49a] G. Simi,[49a,49b] F. Simonetto,[49a,49b] R. Stroili,[49a,49b] S. Akar,[50] E. Ben-Haim,[50] M. Bomben,[50] G. R. Bonneaud,[50] H. Briand,[50] G. Calderini,[50] J. Chauveau,[50] Ph. Leruste,[50] G. Marchiori,[50] J. Ocariz,[50] M. Biasini,[51a,51b] E. Manoni,[51a] S. Pacetti,[51a,51b] A. Rossi,[51a] C. Angelini,[52a,52b] G. Batignani,[52a,52b] S. Bettarini,[52a,52b] M. Carpinelli,[52a,52b,**] G. Casarosa,[52a,52b] A. Cervelli,[52a,52b] M. Chrzaszcz,[52a] F. Forti,[52a,52b] M. A. Giorgi,[52a,52b] A. Lusiani,[52a,52c] B. Oberhof,[52a,52b] E. Paoloni,[52a,52b] A. Perez,[52a] G. Rizzo,[52a,52b] J. J. Walsh,[52a] D. Lopes Pegna,[53] J. Olsen,[53] A. J. S. Smith,[53] F. Anulli,[54a] R. Faccini,[54a,54b] F. Ferrarotto,[54a] F. Ferroni,[54a,54b] M. Gaspero,[54a,54b] L. Li Gioi,[54a] A. Pilloni,[54a,54b] G. Piredda,[54a] C. Bünger,[55] S. Dittrich,[55] O. Grünberg,[55] M. Hess,[55] T. Leddig,[55] C. Voß,[55] R. Waldi,[55] T. Adye,[56] E. O. Olaiya,[56] F. F. Wilson,[56] S. Emery,[57] G. Vasseur,[57] D. Aston,[58] D. J. Bard,[58] C. Cartaro,[58] M. R. Convery,[58] J. Dorfan,[58] G. P. Dubois-Felsmann,[58] W. Dunwoodie,[58] M. Ebert,[58] R. C. Field,[58] B. G. Fulsom,[58] M. T. Graham,[58] C. Hast,[58] W. R. Innes,[58] P. Kim,[58] D. W. G. S. Leith,[58] D. Lindemann,[58] S. Luitz,[58] V. Luth,[58] H. L. Lynch,[58] D. B. MacFarlane,[58] D. R. Muller,[58] H. Neal,[58] M. Perl,[58,*] T. Pulliam,[58] B. N. Ratcliff,[58] A. Roodman,[58] A. A. Salnikov,[58] R. H. Schindler,[58] A. Snyder,[58] D. Su,[58] M. K. Sullivan,[58] J. Va'vra,[58] W. J. Wisniewski,[58] H. W. Wulsin,[58] M. V. Purohit,[59] R. M. White,[59,††] J. R. Wilson,[59] A. Randle-Conde,[60] S. J. Sekula,[60] M. Bellis,[61] P. R. Burchat,[61] E. M. T. Puccio,[61] M. S. Alam,[62] J. A. Ernst,[62] R. Gorodeisky,[63] N. Guttman,[63] D. R. Peimer,[63] A. Soffer,[63] S. M. Spanier,[64] J. L. Ritchie,[65] R. F. Schwitters,[65] B. C. Wray,[65] J. M. Izen,[66] X. C. Lou,[66] F. Bianchi,[67a,67b] F. De Mori,[67a,67b] A. Filippi,[67a] D. Gamba,[67a,67b] L. Lanceri,[68a,68b] L. Vitale,[68a,68b] F. Martinez-Vidal,[69] A. Oyanguren,[69] P. Villanueva-Perez,[69] J. Albert,[70] Sw. Banerjee,[70] A. Beaulieu,[70] F. U. Bernlochner,[70] H. H. F. Choi,[70] G. J. King,[70] R. Kowalewski,[70] M. J. Lewczuk,[70] T. Lueck,[70] I. M. Nugent,[70] J. M. Roney,[70] R. J. Sobie,[70] N. Tasneem,[70] T. J. Gershon,[71] P. F. Harrison,[71] T. E. Latham,[71] H. R. Band,[72] S. Dasu,[72] Y. Pan,[72] R. Prepost,[72] and S. L. Wu[72]

(The *BABAR* Collaboration)

[1]*Laboratoire d'Annecy-le-Vieux de Physique des Particules (LAPP), Université de Savoie, CNRS/IN2P3, F-74941 Annecy-Le-Vieux, France*
[2]*Universitat de Barcelona, Facultat de Fisica, Departament ECM, E-08028 Barcelona, Spain*
[3a]*INFN Sezione di Bari, I-70126 Bari, Italy*
[3b]*Dipartimento di Fisica, Università di Bari, I-70126 Bari, Italy*

[4]University of Bergen, Institute of Physics, N-5007 Bergen, Norway
[5]Lawrence Berkeley National Laboratory and University of California, Berkeley, California 94720, USA
[6]Ruhr Universität Bochum, Institut für Experimentalphysik 1, D-44780 Bochum, Germany
[7]University of British Columbia, Vancouver, British Columbia V6T 1Z1, Canada
[8]Brunel University, Uxbridge, Middlesex UB8 3PH, United Kingdom
[9a]Budker Institute of Nuclear Physics SB RAS, Novosibirsk 630090, Russia
[9b]Novosibirsk State University, Novosibirsk 630090, Russia
[9c]Novosibirsk State Technical University, Novosibirsk 630092, Russia
[10]University of California at Irvine, Irvine, California 92697, USA
[11]University of California at Riverside, Riverside, California 92521, USA
[12]University of California at Santa Barbara, Santa Barbara, California 93106, USA
[13]University of California at Santa Cruz, Institute for Particle Physics, Santa Cruz, California 95064, USA
[14]California Institute of Technology, Pasadena, California 91125, USA
[15]University of Cincinnati, Cincinnati, Ohio 45221, USA
[16]University of Colorado, Boulder, Colorado 80309, USA
[17]Colorado State University, Fort Collins, Colorado 80523, USA
[18]Technische Universität Dortmund, Fakultät Physik, D-44221 Dortmund, Germany
[19]Laboratoire Leprince-Ringuet, Ecole Polytechnique, CNRS/IN2P3, F-91128 Palaiseau, France
[20]University of Edinburgh, Edinburgh EH9 3JZ, United Kingdom
[21a]INFN Sezione di Ferrara, I-44122 Ferrara, Italy
[21b]Dipartimento di Fisica e Scienze della Terra, Università di Ferrara, I-44122 Ferrara, Italy
[22]INFN Laboratori Nazionali di Frascati, I-00044 Frascati, Italy
[23a]INFN Sezione di Genova, I-16146 Genova, Italy
[23b]Dipartimento di Fisica, Università di Genova, I-16146 Genova, Italy
[24]Indian Institute of Technology Guwahati, Guwahati, Assam 781 039, India
[25]Universität Heidelberg, Physikalisches Institut, D-69120 Heidelberg, Germany
[26]Humboldt-Universität zu Berlin, Institut für Physik, D-12489 Berlin, Germany
[27]University of Iowa, Iowa City, Iowa 52242, USA
[28]Iowa State University, Ames, Iowa 50011-3160, USA
[29]Physics Department, Jazan University, Jazan 22822, Kingdom of Saudia Arabia
[30]Johns Hopkins University, Baltimore, Maryland 21218, USA
[31]Laboratoire de l'Accélérateur Linéaire, IN2P3/CNRS et Université Paris-Sud 11, Centre Scientifique d'Orsay, F-91898 Orsay Cedex, France
[32]Lawrence Livermore National Laboratory, Livermore, California 94550, USA
[33]University of Liverpool, Liverpool L69 7ZE, United Kingdom
[34]Queen Mary, University of London, London E1 4NS, United Kingdom
[35]University of London, Royal Holloway and Bedford New College, Egham, Surrey TW20 0EX, United Kingdom
[36]University of Louisville, Louisville, Kentucky 40292, USA
[37]Johannes Gutenberg-Universität Mainz, Institut für Kernphysik, D-55099 Mainz, Germany
[38]University of Manchester, Manchester M13 9PL, United Kingdom
[39]University of Maryland, College Park, Maryland 20742, USA
[40]Massachusetts Institute of Technology, Laboratory for Nuclear Science, Cambridge, Massachusetts 02139, USA
[41]McGill University, Montréal, Québec H3A 2T8, Canada
[42a]INFN Sezione di Milano, I-20133 Milano, Italy
[42b]Dipartimento di Fisica, Università di Milano, I-20133 Milano, Italy
[43]University of Mississippi, University, Mississippi 38677, USA
[44]Université de Montréal, Physique des Particules, Montréal, Québec H3C 3J7, Canada
[45a]INFN Sezione di Napoli, I-80126 Napoli, Italy
[45b]Dipartimento di Scienze Fisiche, Università di Napoli Federico II, I-80126 Napoli, Italy
[46]NIKHEF, National Institute for Nuclear Physics and High Energy Physics, NL-1009 DB Amsterdam, Netherlands
[47]University of Notre Dame, Notre Dame, Indiana 46556, USA
[48]Ohio State University, Columbus, Ohio 43210, USA
[49a]INFN Sezione di Padova, I-35131 Padova, Italy
[49b]Dipartimento di Fisica, Università di Padova, I-35131 Padova, Italy
[50]Laboratoire de Physique Nucléaire et de Hautes Energies, IN2P3/CNRS, Université Pierre et Marie Curie-Paris6, Université Denis Diderot-Paris7, F-75252 Paris, France
[51a]INFN Sezione di Perugia, I-06123 Perugia, Italy
[51b]Dipartimento di Fisica, Università di Perugia, I-06123 Perugia, Italy
[52a]INFN Sezione di Pisa, I-56127 Pisa, Italy
[52b]Dipartimento di Fisica, Università di Pisa, I-56127 Pisa, Italy

[52c]Scuola Normale Superiore di Pisa, I-56127 Pisa, Italy
[53]Princeton University, Princeton, New Jersey 08544, USA
[54a]INFN Sezione di Roma, I-00185 Roma, Italy
[54b]Dipartimento di Fisica, Università di Roma La Sapienza, I-00185 Roma, Italy
[55]Universität Rostock, D-18051 Rostock, Germany
[56]Rutherford Appleton Laboratory, Chilton, Didcot, Oxon OX11 0QX, United Kingdom
[57]CEA, Irfu, SPP, Centre de Saclay, F-91191 Gif-sur-Yvette, France
[58]SLAC National Accelerator Laboratory, Stanford, California 94309 USA
[59]University of South Carolina, Columbia, South Carolina 29208, USA
[60]Southern Methodist University, Dallas, Texas 75275, USA
[61]Stanford University, Stanford, California 94305-4060, USA
[62]State University of New York, Albany, New York 12222, USA
[63]School of Physics and Astronomy, Tel Aviv University, Tel Aviv 69978, Israel
[64]University of Tennessee, Knoxville, Tennessee 37996, USA
[65]University of Texas at Austin, Austin, Texas 78712, USA
[66]University of Texas at Dallas, Richardson, Texas 75083, USA
[67a]INFN Sezione di Torino, I-10125 Torino, Italy
[67b]Dipartimento di Fisica, Università di Torino, I-10125 Torino, Italy
[68a]INFN Sezione di Trieste, I-34127 Trieste, Italy
[68b]Dipartimento di Fisica, Università di Trieste, I-34127 Trieste, Italy
[69]IFIC, Universitat de Valencia-CSIC, E-46071 Valencia, Spain
[70]University of Victoria, Victoria, British Columbia V8W 3P6, Canada
[71]Department of Physics, University of Warwick, Coventry CV4 7AL, United Kingdom
[72]University of Wisconsin, Madison, Wisconsin 53706, USA

(Received 10 February 2015; published 29 April 2015)

We present a search for a neutral, long-lived particle L that is produced in e^+e^- collisions and decays at a significant distance from the e^+e^- interaction point into various flavor combinations of two oppositely charged tracks. The analysis uses an e^+e^- data sample with a luminosity of 489.1 fb^{-1} collected by the *BABAR* detector at the $\Upsilon(4S)$, $\Upsilon(3S)$, and $\Upsilon(2S)$ resonances and just below the $\Upsilon(4S)$. Fitting the two-track mass distribution in search of a signal peak, we do not observe a significant signal, and set 90% confidence level upper limits on the product of the L production cross section, branching fraction, and reconstruction efficiency for six possible two-body L decay modes as a function of the L mass. The efficiency is given for each final state as a function of the mass, lifetime, and transverse momentum of the candidate, allowing application of the upper limits to any production model. In addition, upper limits are provided on the branching fraction $\mathcal{B}(B \to X_s L)$, where X_s is a strange hadronic system.

DOI: 10.1103/PhysRevLett.114.171801 PACS numbers: 13.66.Hk, 14.80.Ec

Recent anomalous astrophysical observations [1–3] have generated interest in GeV-scale hidden-sector states that may be long-lived [4–12]. Searches for long-lived particles have been performed both in the sub-GeV [13–15] and multi-GeV [16–21] mass ranges. Dedicated experiments to search for such particles have been proposed [22] or are under construction [23]. However, the $O(1\ \mathrm{GeV}/c^2)$ mass range has remained mostly unexplored, especially in a heavy-flavor environment. B factories offer an ideal laboratory to probe this regime. Previously, the only B-factory results were from a search for a heavy neutralino by the Belle Collaboration [24].

We search, herein, for a neutral, long-lived particle L, which decays into any of the final states $f = e^+e^-$, $\mu^+\mu^-$, $e^\pm\mu^\mp$, $\pi^+\pi^-$, K^+K^-, or $K^\pm\pi^\mp$. A displaced vertex and two-body decay kinematics constitute the main means for background suppression, and the search is performed by fitting the distribution of the L-candidate mass.

The results are presented in two ways. In the "model-independent" presentation, no assumption is made regarding the production mechanism of the L. Rather, we present limits on the product of the inclusive production cross section $\sigma(e^+e^- \to LX)$, branching fraction $\mathcal{B}(L \to f)$, and efficiency $\epsilon(f)$ for each of the two-body final states f, where X is any set of particles. As Supplemental Material to this Letter [25], we provide tables of the efficiency as a function of L mass m, transverse [26] momentum p_T in the center-of-mass (c.m.) frame, and proper decay distance $c\tau$, assuming the L to be a spin-zero particle. The provided upper limits, efficiencies, and p_T distributions of the simulated events used to obtain the efficiencies facilitate the application of the model-independent presentation of the results to any specific model of L production. In the "model-dependent" presentation, we provide limits on the branching fraction for the decay $B \to X_s L$, where X_s is a hadronic system with strangeness -1. This presentation is

motivated by Higgs-portal models of dark matter and other hidden sectors [8–11].

The data were collected with the *BABAR* detector at the PEP-II asymmetric-energy e^+e^- collider at SLAC National Accelerator Laboratory. The sample consists of 404.0 ± 1.7 fb^{-1} collected at a c.m. energy corresponding to the $\Upsilon(4S)$ resonance, an "off-resonance" sample of 43.74 ± 0.20 fb^{-1} collected about 40 MeV below the $\Upsilon(4S)$ peak, 27.85 ± 0.18 fb^{-1} collected at the $\Upsilon(3S)$, and 13.56 ± 0.09 fb^{-1} taken at the $\Upsilon(2S)$ [27]. The $\Upsilon(4S)$ sample contains $(448.4 \pm 2.2) \times 10^6$ $B\bar{B}$ pairs, and the $\Upsilon(3S)$ and $\Upsilon(2S)$ samples have $(121.3 \pm 1.2) \times 10^6$ $\Upsilon(3S)$ and $(98.3 \pm 0.9) \times 10^6$ $\Upsilon(2S)$ mesons, respectively [28]. An additional $\Upsilon(4S)$ sample of 20.37 ± 0.09 fb^{-1} is used to validate the analysis procedure and is not included in the final analysis.

The *BABAR* detector and its operation are described in detail in Refs. [29] and [30]. Charged-particle momenta are measured in a tracking system consisting of a five-layer, double-sided silicon vertex detector (SVT) and a 40-layer drift chamber (DCH), both located in a 1.5 T axial magnetic field. Electron and photon energies are measured in a CsI (Tl) electromagnetic calorimeter (EMC) inside the magnet coil. Charged-particle identification (PID) is performed using an internally reflecting, ring-imaging Cherenkov detector, as well as the energy loss measured by the SVT, DCH, and EMC. Muons are identified mainly with the instrumented magnetic-flux return.

Using Monte Carlo (MC) simulations, we determine both the signal mass resolution and reconstruction efficiency. The events are produced with the EVTGEN [31] event generator, taking the L spin to be zero. We generate two types of signal MC samples. In the first type, which is used to create the efficiency tables [25] for the model-independent presentation, the L is produced at 11 different masses, $m_0^{\rm MC} = 0.5$, 1, 2, 3, 4, 5, 6, 7, 8, 9, and 9.5 GeV/c^2. For $m_0^{\rm MC} \leq 4$ GeV/c^2, the L is created in the process $e^+e^- \to B\bar{B}$, with one B meson decaying to $L + N\pi$ ($N = 1$, 2, or 3) and the other B decaying generically. At higher masses, the production process is $\Upsilon(4S) \to L + N\pi$. In both cases, the L is produced uniformly throughout the available phase space, with an average transverse decay distance of 20 cm. The events are subsequently reweighted to obtain efficiencies for other decay lengths. Note that these specific processes do not reflect preferred hypotheses about the production mechanism, nor do the results depend on these processes. Rather, they are a convenient method to populate the kinematic range for the efficiency tables.

The second type of signal MC sample, used for the model-dependent presentation of the results, contains $B \to X_s L$ decays, for the seven mass values $m_0^{\rm MC} = 0.5$, 1, 2, 3, 3.5, 4, and 4.5 GeV/c^2. The X_s is nominally taken to be 10% K, 25% $K^*(892)$, and 65% $K^*(1680)$ [32], with the high-mass tail of the X_s spectrum suppressed by phase-space limitations, especially for heavy L states. This choice of X_s composition results in an L-momentum spectrum as a function of $m_0^{\rm MC}$ that reproduces the dimuon spectrum for $B \to X_s \mu^+\mu^-$ in events generated with EVTGEN using the BTOXSLL model [31]. The other B meson in the event decays generically.

In addition to the signal MC samples, background MC samples are used for optimizing the event selection criteria and studying the signal extraction method. The background samples are $e^+e^- \to B\bar{B}$ (produced with EVTGEN [31]), $\tau^+\tau^-$, $\mu^+\mu^-$ (KK2F [33]), e^+e^- (BHWIDE [34]), and $q\bar{q}$ events (JETSET [35]), where q is a u, d, s, or c quark. The detector response is simulated with GEANT4 [36].

The L candidates are reconstructed from pairs of oppositely charged tracks, identified as either e^+e^-, $\mu^+\mu^-$, $e^\pm\mu^\mp$, $\pi^+\pi^-$, K^+K^-, or $K^\pm\pi^\mp$. The PID efficiency depends on the track momentum, and is in the range 0.96–0.99 for electrons, 0.60–0.88 for muons, and 0.90–0.98 for kaons and pions. The pion misidentification probability is less than 0.01 for the electron PID criteria, less than 0.03 for the muon criteria, and averages at 0.06 for the kaon criteria. A track may have different PID assignments and may appear in multiple pairs. Each track must satisfy $d_0/\sigma_{d_0} > 3$, where d_0 is the transverse distance of closest approach of the track to the e^+e^- interaction point (IP), and σ_{d_0} is the d_0 uncertainty, calculated from the SVT and DCH hit position uncertainties during the track reconstruction. The two tracks are fit to a common vertex, and the χ^2 value of the fit is required to be smaller than 10 for one degree of freedom. The two-dimensional vector $\vec{r}$ between the IP and the vertex in the transverse plane must have length $r \equiv |\vec{r}|$ in the range $1 < r < 50$ cm, and the uncertainty on r is required to satisfy $\sigma_r < 0.2$ cm. We require the angle α between $\vec{r}$ and the L-candidate transverse-momentum vector to satisfy $\alpha < 0.01$ rad. The uncertainty σ_m on the measured L-candidate mass m must be less than 0.2 GeV/c^2. The L candidate is discarded if either of the tracks has SVT or DCH hits located between the IP and the vertex, or if the vertex is within the material of the beam pipe wall, the DCH support tube, or the DCH inner cylinder. Candidates must satisfy the following decay-mode-specific invariant-mass criteria: $m_{e^+e^-} > 0.44$ GeV/c^2, $m_{\mu^+\mu^-} < 0.37$ GeV/c^2 or $m_{\mu^+\mu^-} > 0.5$ GeV/c^2, $m_{e^\pm\mu^\mp} > 0.48$ GeV/c^2, $m_{\pi^+\pi^-} > 0.86$ GeV/c^2, $m_{K^+K^-} > 1.35$ GeV/c^2, and $m_{K^\pm\pi^\mp} > 1.05$ GeV/c^2. These criteria reject background from $K_S^0 \to \pi^+\pi^-$ and $\Lambda \to p\pi^-$ decays. In addition, other than in the $\mu^+\mu^-$ mode, they exclude low-mass regions in which the mass distributions of background MC events are not smooth and, therefore, are incompatible with the background description method outlined below. We require at least one of the tracks of $L \to \mu^+\mu^-$ candidates with $m \geq 8$ GeV/c^2 to have an SVT hit. This rejects candidates that decay into $\mu^+\mu^-$ within the material of the final-focusing magnets and, thus, have poor mass resolution. These selection criteria are

found to yield near-optimal signal sensitivity given the broad range of m and r values of this search.

For each decay mode, we determine the full efficiency ϵ, including the impact of detector acceptance, trigger, reconstruction, and selection criteria, for different values of $m_0^{\rm MC}$, $c\tau$, and p_T. The efficiency, which is tabulated in Ref. [25], reaches a maximal value of $\epsilon = 52\%$ for $L \to \pi^+\pi^-$ decays with $m = 2$ GeV/c^2, $p_T > 4$ GeV/c, and $c\tau = 6$ cm. The dominant factor affecting ϵ is the average transverse flight distance $\langle r\rangle = c\tau\langle p_T\rangle/m$. Reflecting the $1 < r < 50$ cm requirement, ϵ drops rapidly when $\langle r\rangle$ goes below 1 cm or above 50 cm. In addition, ϵ has some dependence on the L polar-angle θ, measured with respect to the direction of the e^+e^- center of mass. For a $1 + \cos^2\theta$ distribution in the c.m. frame, the strongest dependence is observed for track momentum $p < 0.3$ GeV/c, where ϵ is decreased by 22% relative to that of a uniform $\cos\theta$ distribution. For $p > 2$ GeV/c, ϵ varies by no more than 8%. Similarly, the efficiency depends weakly on whether L is a scalar or a vector particle. For a longitudinally polarized vector, ϵ typically varies by a few percent relative to the scalar case, with the greatest impact being an efficiency reduction of 25% for $p_T < 0.3$ GeV/c, $m = 7$ GeV/c^2.

The dominant source of background consists of hadronic events with high track multiplicity, where large-d_0 tracks originate mostly from K_S^0, Λ, $K^\pm$, and $\pi^\pm$ decays, as well as particle interactions with detector material. Random overlaps of such tracks comprise the majority of the background candidates.

We extract the signal yield for each final state as a function of L mass with unbinned extended maximum-likelihood fits of the m distribution. The procedure is based on the fact that signal MC events peak in m while the background distribution varies slowly. The fit probability density functions (PDFs) for signal and background are constructed separately for each mode and each data sample. The PDFs account for the signal mass resolution, which is evaluated separately in each of 11 mass regions, where each region straddles the $m_0^{\rm MC}$ value of one of the signal MC samples of the first type. In region i, the value of the signal PDF for a candidate with hypothesis mass m_0, measured mass m, and mass resolution uncertainty σ_m is $P_S^i(m) = H_S^i[(m - m_0)/\sigma_m]$, where $H_S^i(x)$ is the histogram of the mass pull $x = (m^{\rm MC} - m_0^{\rm MC})/\sigma_m^{\rm MC}$ for signal MC events of true mass $m_0^{\rm MC}$, measured mass $m^{\rm MC}$, and $m^{\rm MC}$ uncertainty $\sigma_m^{\rm MC}$. This PDF accounts correctly for the large variation in σ_m with r and m.

The background PDF $P_B(m)$ is obtained from the data, so as not to rely on the background simulation, with the following procedure. First, we create a variable-bin-width histogram $H_D(m)$ of the data m distribution. The width of a histogram bin, whose lower edge is in m region i, is $w_i = nR_i$, where $n = 15$, and R_i is the rms width of the signal $m - m_0^{\rm MC}$ distribution in that region. The value of R_i ranges from about 6 MeV/c^2 for $m_0^{\rm MC} = 0.5$ GeV/c^2 to 180 MeV/c^2 for $m_0^{\rm MC} = 9.5$ GeV/c^2. We obtain $P_B(m)$ by fitting $H_D(m)$ with a second-order polynomial spline, with knots located at the bin boundaries. Simulation studies of the background mass distribution show that the choice $n = 15$ is sufficiently large to prevent $P_B(m)$ from conforming to signal peaks and, thus, hiding statistically significant signals, yet sufficiently small to avoid high false-signal yields due to background fluctuations. Figure 1 shows the m distributions of the data (with uniform mass bins) and the background PDFs.

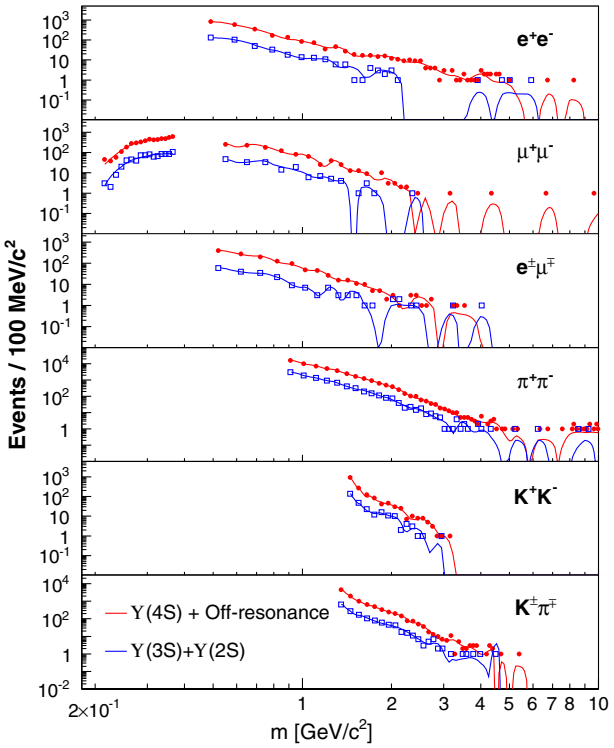

FIG. 1 (color online). Mass distribution of the $\Upsilon(4S) +$ off-resonance data (red solid points) and $\Upsilon(3S) + \Upsilon(2S)$ data (blue open squares) for each mode, overlaid with the background PDF P_B in matching color. In the $\mu^+\mu^-$ mode, the bin width in the range $m < 370$ MeV/c^2 is 10 MeV/c^2.

We scan the data in search of an L signal, varying m_0 in steps of 2 MeV/c^2. At each scan point, we fit the data in the full mass range using the PDF $n_S P_S + n_B P_B$, where the signal and background yields n_S and n_B are determined in the fit. The statistical significance $S = \text{sign}(n_S)\sqrt{2\log(\mathcal{L}_S/\mathcal{L}_B)}$, where $\mathcal{L}_S$ is the maximum likelihood for n_s signal events over the background yield, and $\mathcal{L}_B$ is the likelihood for $n_S = 0$, is calculated for each scan point. The distributions of S values for all the scan points are nearly normal.

Significance values greater than 3 are found in two scan points, both in the $\mu^+\mu^-$ mode in the $\Upsilon(4S) +$ off-resonance sample. The highest significance is $S = 4.7$, with a signal yield of 13 events at the low-mass threshold of $m_0 = 0.212$ GeV/c^2. The second-highest significance of $S = 4.2$ occurs at $m_0 = 1.24$ GeV/c^2,

corresponding to a signal yield of 10 events. To obtain the p values for these significances, we perform the scans on a large number of $m_{\mu^+\mu^-}$ spectra generated according to the background PDF, obtained from the data with a finer binning of $n = 5$. With this choice of n, the generated spectra are not sensitive to fluctuations of the order of the signal resolution (which correspond to $n = 1$), yet include features that are much smaller than the resolution of the PDF ($n = 15$). We find that the probability for $S \geq 4.7$ (4.2) anywhere in the $\mu^+\mu^-$ spectrum with $m_{\mu^+\mu^-} < 0.37\,\mathrm{GeV}/c^2$ ($m_{\mu^+\mu^-} > 0.5\,\mathrm{GeV}/c^2$) is 4×10^{-4} (8×10^{-3}). The p values are consistent with the naive expectation $p(S)w/R$, where $p(S)$ is the p value without the "look-elsewhere effect," w is the width of the mass region under study, and R is the average value of R_i. We do not include the other modes in the calculation of the p values. Doing so would naively multiply the p values by about six. Further study provides strong indication for material-interaction background in the $0.212\ \mathrm{GeV}/c^2$ region. Specifically, most of the 34 $\mu^+\mu^-$ vertices with $m_{\mu^+\mu^-} < 0.215\ \mathrm{GeV}/c^2$ occur inside or at the edge of detector-material regions, including 10 of the vertices that also pass the e^+e^- selection criteria and 10 that pass the $\pi^+\pi^-$ criteria. Thus, the peak is consistent with misidentified photon conversions and hadronic interactions close to the mass threshold. We conclude that a significant signal is not observed.

Systematic uncertainties on the signal yields are calculated for each scan fit separately. The dominant uncertainty is due to the background PDF, and is evaluated by repeating the scans with $n = 20$, which is the maximal plausible value for n that does not lead to a large probability for false-signal detection. This uncertainty is a few signal events on average, and generally decreases with mass. An additional uncertainty is evaluated by taking R_i from events with $p_T < 0.8\ \mathrm{GeV}/c$ or $p_T > 0.8\ \mathrm{GeV}/c$. To estimate uncertainties due to the weak signal PDF dependence on r and m, we repeat the scans after obtaining H_S^i from signal MC events with either $r < 4$ cm or $r > 4$ cm, as well as from signal MC events from adjacent mass regions. The uncertainty due to the signal mass resolution is evaluated by comparing the mass pull distributions of K_S^0 mesons in data and MC, whose widths differ by 5%. A conservative uncertainty of 2% on the signal reconstruction efficiencies is estimated from the K_S^0 reconstruction efficiency in data and MC. Smaller uncertainties on the efficiency, of up to 1%, arise from particle identification and the finite size of the signal MC sample. The total uncertainties on the efficiency are reported in the efficiency tables [25].

Observing that the likelihood $\mathcal{L}_S$ is a nearly normal function of the signal yield, it is analytically convolved with a Gaussian representing the systematic uncertainties in n_S, obtaining the modified likelihood function $\mathcal{L}'_S$. The 90% confidence level upper limit U_S on the signal yield is calculated from $\int_0^{U_S} \mathcal{L}' dn_S / \int_0^{\infty} \mathcal{L}' dn_S = 0.9$. Dividing U_S

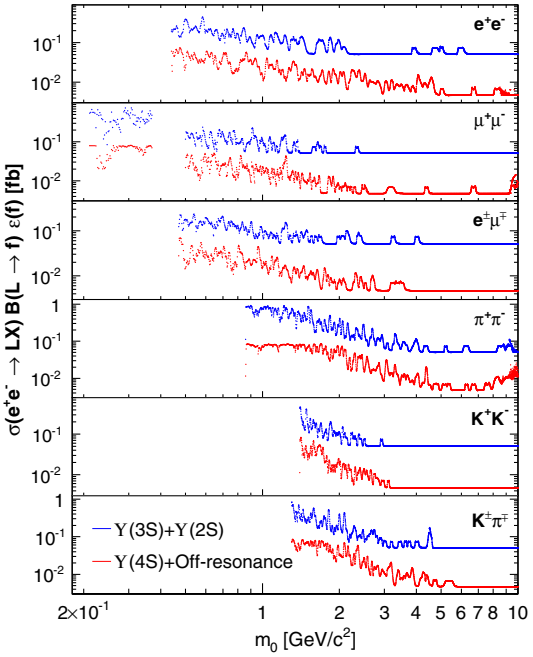

FIG. 2 (color online). The 90% confidence level upper limits on $\sigma(e^+e^- \to LX)\mathcal{B}(L \to f)\epsilon(f)$ as a function of L mass for the $\Upsilon(4S)$ + off-resonance sample (red lower points) and for the $\Upsilon(3S) + \Upsilon(2S)$ sample (blue upper points). The limits include the systematic uncertainties on the signal yield.

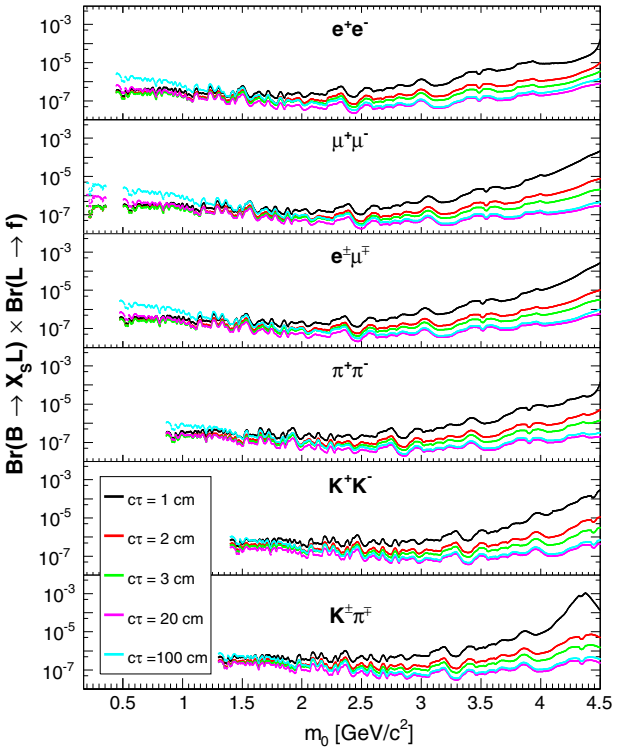

FIG. 3 (color online). Implications of the results for Higgs-portal scenarios, showing the 90% confidence level upper limits on the product of branching fractions $\mathcal{B}(B \to X_s L)\mathcal{B}(L \to f)$ as a function of L mass for each final state f and for different values of $c\tau$. The limits include all systematic uncertainties.

by the luminosity yields an upper limit on the product $\sigma(e^+e^- \to LX)\mathcal{B}(L \to f)\epsilon(f)$. This limit is shown for each mode as a function of m_0 in Fig. 2, and given in the Supplemental Material [25].

Determining the efficiency from the $B \to X_s L$ signal MC sample, we obtain upper limits on the product of branching fractions $\mathcal{B}(B \to X_s L)\mathcal{B}(L \to f)$ for each of the final states f. These limits are shown in Fig. 3.

In conclusion, we have performed a search for long-lived particles L produced in e^+e^- collisions. No signal is observed, and upper limits on $\sigma(e^+e^- \to LX)\mathcal{B}(L \to f)\epsilon(f)$ and on $\mathcal{B}(B \to X_s L)\mathcal{B}(L \to f)$ are set at 90% confidence level for six two-body final states f. We provide detailed efficiency tables to enable application of our results to any specific model [25].

We are grateful for the excellent luminosity and machine conditions provided by our PEP-II2 colleagues, and for the substantial dedicated effort from the computing organizations that support *BABAR*. The collaborating institutions wish to thank SLAC for its support and kind hospitality. This work is supported by DOE and NSF (USA), NSERC (Canada), CEA and CNRS-IN2P3 (France), BMBF and DFG (Germany), INFN (Italy), FOM (The Netherlands), NFR (Norway), MES (Russia), MINECO (Spain), STFC (United Kingdom), BSF (USA-Israel). Individuals have received support from the Marie Curie EIF (European Union) and the A. P. Sloan Foundation (USA).

[*] Deceased.
[†] Present address: University of Tabuk, Tabuk 71491, Saudi Arabia.
[‡] Also at: Università di Perugia, Dipartimento di Fisica, I-06123 Perugia, Italy.
[§] Present address: Laboratoire de Physique Nucléaire et de Hautes Energies, IN2P3/CNRS, F-75252 Paris, France.
[‖] Present address: University of Huddersfield, Huddersfield HD1 3DH, United Kingdom.
[¶] Present address: University of South Alabama, Mobile, AL 36688, USA.
[**] Also at: Università di Sassari, I-07100 Sassari, Italy.
[††] Present address: Universidad Técnica Federico Santa Maria, 2390123 Valparaiso, Chile.

[1] M. Aguilar *et al.* (AMS Collaboration), Phys. Rev. Lett. **110**, 141102 (2013).
[2] O. Adriani *et al.* (PAMELA Collaboration), Nature (London) **458**, 607 (2009).
[3] M. Ackermann *et al.* (Fermi LAT Collaboration), Phys. Rev. Lett. **108**, 011103 (2012).
[4] B. Batell, M. Pospelov, and A. Ritz, Phys. Rev. D **79**, 115008 (2009).
[5] R. Essig, P. Schuster, and N. Toro, Phys. Rev. D **80**, 015003 (2009).
[6] F. Bossi, Adv. High Energy Phys. **2014**, 1 (2014).
[7] P. Schuster, N. Toro, and I. Yavin, Phys. Rev. D **81**, 016002 (2010).
[8] F. Bezrukov and D. Gorbunov, J. High Energy Phys. 07 (2013) 140.
[9] C. Cheung and Y. Nomura, J. High Energy Phys. 11 (2010) 103.
[10] K. Schmidt-Hoberg, F. Staub, and M. W. Winkler, Phys. Lett. B **727**, 506 (2013).
[11] J. D. Clarke, R. Foot, and R. R. Volkas, J. High Energy Phys. 02 (2014) 123.
[12] A. E. Nelson and J. Scholtz, Phys. Rev. D **91**, 014009 (2015).
[13] S. Andreas, C. Niebuhr, and A. Ringwald, Phys. Rev. D **86**, 095019 (2012).
[14] S. N. Gninenko, Phys. Rev. D **85**, 055027 (2012).
[15] T. Adams *et al.* (NuTeV Collaboration), Phys. Rev. Lett. **87**, 041801 (2001).
[16] V. M. Abazov *et al.* (D0 Collaboration), Phys. Rev. Lett. **97**, 161802 (2006).
[17] V. M. Abazov *et al.* (D0 Collaboration), Phys. Rev. Lett. **103**, 071801 (2009).
[18] F. Abe *et al.* (CDF Collaboration), Phys. Rev. D **58**, 051102 (1998).
[19] G. Aad *et al.* (ATLAS Collaboration), Phys. Lett. B **720**, 277 (2013).
[20] G. Aad *et al.* (ATLAS Collaboration), Phys. Rev. Lett. **108**, 251801 (2012).
[21] G. Aad *et al.* (ATLAS Collaboration), Phys. Lett. B **719**, 280 (2013).
[22] R. Essig, P. Schuster, N. Toro, and B. Wojtsekhowski, J. High Energy Phys. 02 (2011) 1.
[23] O. Moreno (HPS Collaboration), arXiv:1310.2060.
[24] D. Liventsev *et al.* (Belle Collaboration), Phys. Rev. D **87**, 071102 (2013).
[25] See Supplemental Material at http://link.aps.org/supplemental/10.1103/PhysRevLett.114.171801 for the efficiency tables.
[26] The term "transverse" refers throughout this Letter to projections of vectors onto the plane transverse to the direction of the e^+e^- center of mass system.
[27] J. P. Lees *et al.* (*BABAR* Collaboration), Nucl. Instrum. Methods Phys. Res., Sect. A **726**, 203 (2013).
[28] G. D. McGregor, Report No. SLAC-R-912, 2008.
[29] B. Aubert *et al.* (*BABAR* Collaboration), Nucl. Instrum. Methods Phys. Res., Sect. A **479**, 1 (2002).
[30] B. Aubert *et al.* (*BABAR* Collaboration), Nucl. Instrum. Methods Phys. Res., Sect. A **729**, 615 (2013).
[31] D. J. Lange, Nucl. Instrum. Methods Phys. Res., Sect. A **462**, 152 (2001).
[32] J. Beringer *et al.* Particle Data Group, Phys. Rev. D **86**, 010001 (2012) and 2013 partial update for the 2014 edition.
[33] S. Jadach, B. F. L. Ward, and Z. Was, Phys. Rev. D **63**, 113009 (2001).
[34] S. Jadach, W. Placzek, and B. F. L. Ward, Phys. Lett. B **390**, 298 (1997).
[35] T. Sjostrand, Comput. Phys. Commun. **82**, 74 (1994).
[36] S. Agostinelli *et al.* (GEANT4 Collaboration), Nucl. Instrum. Methods Phys. Res., Sect. A **506**, 250 (2003).